Analysis of X/R Ratio Effect on Stability of Grid-Following and Grid-Forming Converters

Gao, Xian; Zhou, Dao; Anvari-Moghaddam, Amjad; Blaabjerg, Frede

Published in:
Proceedings of the 2023 IEEE 17th International Conference on Compatibility, Power Electronics and Power Engineering (CPE-POWERENG)

DOI (link to publication from Publisher):
10.1109/CPE-POWERENG58103.2023.10227503

Publication date:
2023

Document Version
Accepted author manuscript, peer reviewed version

Analysis of X/R Ratio Effect on Stability of Grid-Following and Grid-Forming Converters

Xian Gao, Dao Zhou, Amjad Anvari-Moghaddam, Frede Blaabjerg
AAU Energy
Aalborg University
Aalborg, Denmark
xiga@energy.aau.dk, zda@energy.aau.dk, aam@energy.aau.dk, fbl@energy.aau.dk

***Abstract*—The power system is undergoing significant changes with the increasing integration of renewable energy sources, such as wind and solar. The high penetration of these renewable energy sources has posed new challenges on the stability of the power grid. In response to these challenges, grid-following and grid-forming converters have been introduced as an effective solution for the modern power system. However, the impact of the X/R ratio on the stability of these converters is not well understood. In order to fill in this gap, this paper conducts a detailed analysis on the control schemes of both the grid-following and grid-forming converters, and analyzes the eigenvalue trajectories with the change of the X/R ratio. To investigate how the X/R ratio affects the stability of the grid-following and grid-forming converters, a time-domain simulation model is built in Matlab/Simulink. The result reveals that the stability of both the grid-following converter and the grid-forming converter is improved with the decrease of the X/R ratio.**

Keywords — Renewable energy sources, grid-following converters, grid-forming converters, X/R ratio

I. INTRODUCTION

Along with de-carbonization, the penetration of power electronic converters increases, and the traditional power system transforms into a power electronic-based power system, which may create new challenges on the stability of power systems. Grid-following (GFL) converters and grid-forming (GFM) converters are two typical types of power electronic converters, which are widely applied in the power grid with high-penetration renewable energy sources.

As the integration of renewable energy sources and decentralized energy resources increases, the modern power system are becoming more and more complex. The stability analysis accordingly becomes more and more complicated. The stability analysis of the power system is a multi-faceted issue that requires careful consideration of various factors, including the grid strength, parameters of the controllers, as well as the X/R ratio of the feeders. The X/R ratio is defined as the ratio of reactance to resistance of the connecting lines.

Many papers have analyzed the effects of the grid strength and parameters of the controllers on the stability of both the GFL and GFM converters. The effect of the grid strength on the stability of the GFL and GFM converters is analyzed in detail in [1]. It reveals that the GFL converter is more suitable for a strong power grid, while the GFM converter is more suitable for a weak power grid. The effect of the control parameters of both the outer control loop and inner control loop on the voltage-source converters is analyzed in [2] and [3]. The effect of the inner control loop's bandwidth on the GFM control is analyzed in [4]. The effect of different parameters of the AC voltage magnitude controller, virtual admittance controller and current controller on the stability of the GFM converter is analyzed in [5]. It reveals that the increase of the integral gain of the AC voltage magnitude controller and the proportional gain of the current controller can improve the stability of the system.

However, the stability of the GFL and GFM converters considering the effect of the X/R ratio is not well understood. In [6] and [7], the single-input and single-output transfer function is adopted to analyze the relationship between the X/R ratio and the stability. The maximum power transfer capability of grid-connected systems with various X/R ratios at the rated voltage is analyzed in [8]. However, these studies just focus on the GFL converters. The further research is needed to analyze the impact of the X/R ratio on the stability of the GFM converters and some comparisons should be drawn between the GFL and GFM converters.

The stability of a power system can be evaluated through several well-known methods, including the state-space method and impedance model [9], [10]. The eigenvalue analysis method, which is based on the linearized state-space model of the system at its steady-state operation point, can provide precise assessments. This method involves creating a state-space model and examining the distribution of the eigenvalues on the complex plane to make a judgment. The impedance model divides the system into smaller subsystems, and then the Nyquist stability criterion is used to determine if the impedance ratio between the grid impedance and converter impedance is stable or not. Because each subsystem is separate, any changes in one subsystem's parameters do not impact the other subsystems and there's no need to re-establish the model of the whole system. Thus, this method allows for easy updates of the model in the event of any changes to parameters in any of the subsystems.

In order to get an accurate analysis, the eigenvalue analysis method based on the state-space model is adopted in this paper. The objective of this study is to evaluate the effect of the X/R ratio on the stability of GFL and GFM converters in the power electronic-based power system. The main contributions of this paper can be summarized as follows. 1) The controllers of the GFL converter and the GFM converter are depicted in detail. 2) The eigenvalue trajectories are drawn based on the state-space matrixes for a comprehensive stability analysis. 3) The time-domain simulation is established and used for the assessment drawn from the theoretical analysis.

The rest of the paper is organized as follows. In Section II, the control schemes of both the GFL converter and the GFM converter are illustrated in detail. In Section III, the eigenvalue

trajectories are drawn to analyze the effect of the X/R ratio on the stability of the GFL and GFM converters under both the weak and strong power grids. In Section IV, a time-domain simulation model is built in Matlab/Simulink to verify the results of the theoretical stability analysis. Finally, some conclusions are drawn in Section V.

II. Basic Principle of the Grid-Connected Converter

The typical topology of the grid-connected three-phase converter is shown in Fig. 1. L_f and C_f represent the inductor and capacitor of the LC filter, respectively. Z_g represents the grid impedance and it can be given as $Z_g=R_g+j\omega L_g$, where R_g and L_g represent the resistance and the inductance of the power grid, respectively; ω represents the angular frequency of the power grid; j represents the imaginary unit; u_{dc} represents the voltage of the dc-link; u_a, u_b and u_c represent the output voltages of the converter; u_{pcca}, u_{pccb} and u_{pccc} represent the voltages at the point of common coupling (PCC); i_a, i_b and i_c represent the output currents of the converter; i_{ga}, i_{gb} and i_{gc} represent the currents of the power grid; i_{Ca}, i_{Cb} and i_{Cc} represent capacitor currents.

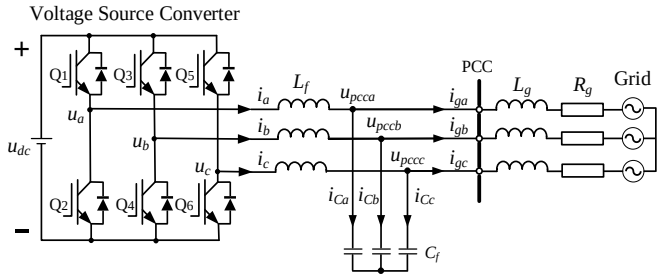

Fig. 1. Typical topology of the grid-connected three-phase converter.

According to the operation modes, synchronization methods with the power grid and the control schemes, the power electronic converters can be divided into two types [11]. One is the GFL converter and the other is the GFM converter.

A. Grid-following converter

The GFL converters are widely applied in power systems which have a high penetration of renewable energy sources. They inject the active power and reactive power into the power grid through regulating the currents. They cannot provide the voltage and frequency references for the power grid. The active power and reactive power control, which is known as PQ control, is adopted in this paper. The typical control scheme of the GFL converter is shown in Fig. 2. The references of the active and reactive power are represented as P_{ref} and Q_{ref}, respectively. The output active and reactive power are represented as P_e and Q_e, respectively. K_C is the proportional coefficient of the capacitor current feedback.

As shown in Fig. 2, the GFL converter consists of an outer power control loop, an inner current control loop and a phase-locked loop (PLL). Moreover, an active damping method is utilized to reduce the resonant peak while maintaining the efficiency of the converter. The GFL control realizes synchronizing with the power grid through the PLL unit. It is worth noting that a moving average filter (MAF) based PLL is adopted to improve the performance of the GFL converter under the weak power grid [12]. In steady-state conditions, the PLL unit can precisely monitor the phase of the PCC voltage. However, the introduction of small perturbations to the PCC voltage leads to a slight variance between the control synchronizing frame established by the PLL unit and the actual system synchronizing frame established by the PCC voltage [13]. The relationship between the two synchronizing frames can be given as:

$$\begin{bmatrix}\Delta x_d^c\\ \Delta x_q^c\end{bmatrix}=\begin{bmatrix}\Delta x_d^s\\ \Delta x_q^s\end{bmatrix}+\begin{bmatrix}X_{q0}\\ -X_{d0}\end{bmatrix}\cdot\Delta\theta \tag{1}$$

where the variables in the actual synchronizing frame are represented with superscript s, while the variables in the control synchronizing frame are represented with superscript c; the small disturbance of variables are denoted with the prefix Δ and the steady-state values of variables are denoted with subscript 0; the d-axis and q-axis components of variables are denoted with subscripts d and q, respectively.

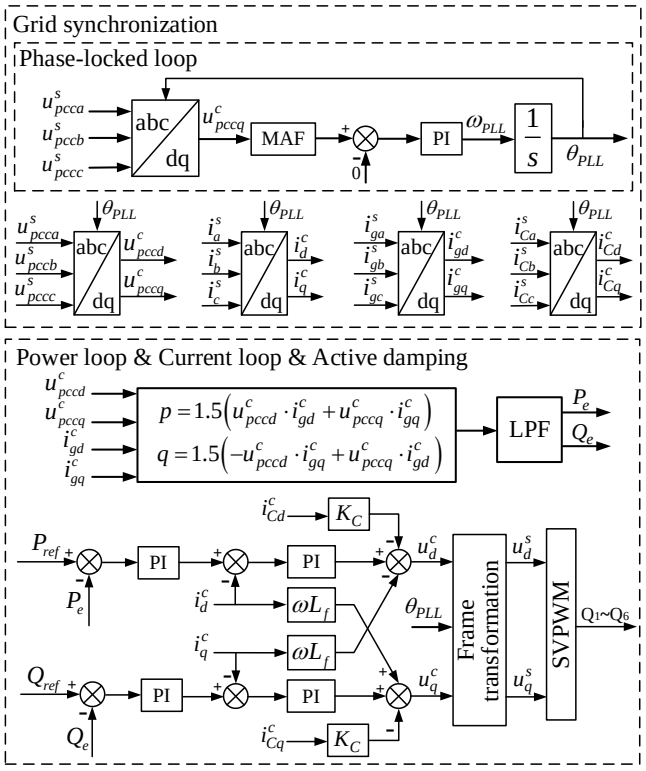

Fig. 2. The control scheme of the grid-following (GFL) converter.

B. Grid-forming converter

The GFM converter is an effective way to cope with the stability problems of the power electronic-based power systems. It doesn't need a PLL unit to synchronize with the power grid which is commonly used in the GFL converters. Instead, the GFM converters can realize self-synchronization, which allows them to form a stable grid and operate in an islanded mode without the need for an extra voltage source or the power grid. The GFM converters can also provide the regulations of the voltage and the frequency for the power grid. This makes GFM converters a useful tool for integrating renewable energy sources into the power grid, as they are able to provide stable and reliable power without relying on traditional synchronous generators.

In traditional power systems, synchronous generators maintain the grid stability through their inherent properties, including inertia and voltage regulation. However, renewable energy sources, such as solar and wind power, lack these characteristics and can sometimes destabilize the grid. In order to overcome these limitations, the virtual synchronous generator (VSG) control has been emerging, which aims to

provide the renewable energy source with the same characteristics as a synchronous generator.

The VSG control is adopted as the typical GFM control in this paper and the control scheme is shown in Fig. 3. *J* denotes the emulated moment of inertia and the damping coefficient is represented as *D*. k_q represents the integrity coefficient and k_u represents the voltage droop coefficient; ω_g represents the rated grid angular frequency; E_m and θ_{VSG} represent the amplitude and phase angle of the reference voltage, respectively; E_0 represents the no-load electromotive force of the converter; U_N represents the peak value of the rated grid voltage.

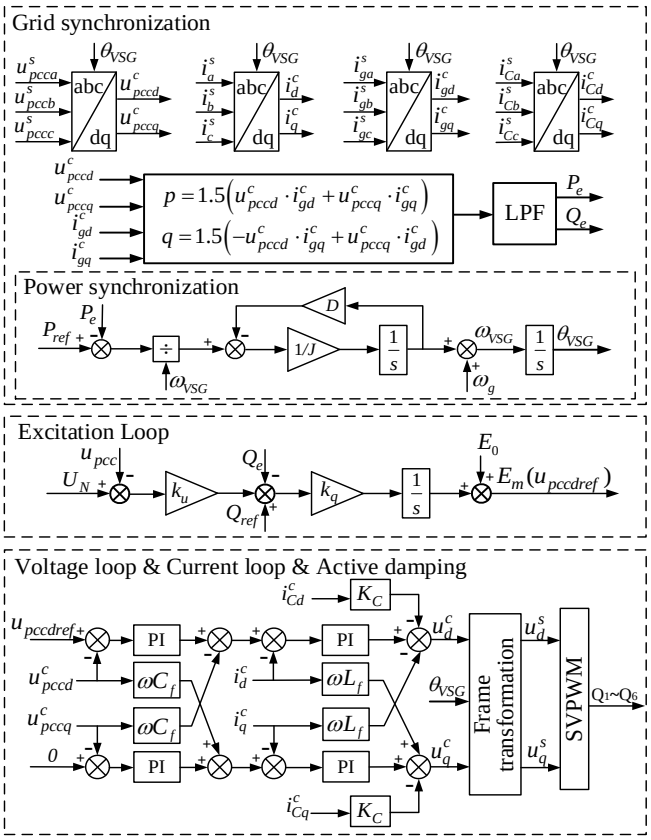

Fig. 3. The control scheme of the grid-forming (GFM) converter.

As shown in Fig. 3, the GFM control consists of the power synchronization loop, excitation loop, outer voltage control loop and inner current control loop. It is worth pointing out that the difference between the actual system synchronizing frame and the control synchronizing frame is due to the power synchronization loop.

III. Analysis Based on the Eigenvalue Trajectories

Many papers have analyzed the effects of the short-circuit ratio (SCR) on the stability of the GFL and GFM converters [14]. SCR is used to represent the grid strength. When the SCR is less than 3, the power grid is considered weak. When the SCR is larger than 3, the power grid is considered strong [15]. However, there are few papers focusing on the analysis of the relationship between the X/R ratio and the stability of the converters. In order to fill in this gap, the analysis based on the state-space method is conducted in this paper.

As for the medium voltage distribution feeders, the X/R ratio is greater than 1, whereas for the low voltage distribution feeders, the X/R ratio is less than 1. Most analysis about the effect of the grid impedance on the stability of the converters is based on the assumption that X≫R. However, when the converter is connected to an extremely weak power grid, the assumption may not be satisfied due to the large resistance of the low voltage power system. Thus, the effect of the X/R ratio on the stability deserves to be further analyzed.

A case study of the 1.5 kW grid-connected converter is built for the stability analysis and the key parameters are listed in TABLE I. Moreover, both the weak and strong power grids are discussed in this paper. The SCR is set as 2.5 and 10 for this case study and the X/R ratio is ranged from 0.1 to 10.

Based on the detailed control schemes of the GFL and GFM converters illustrated in Section II, it is easy to obtain the linearized state-space models of both the GFL and GFM converters. Then, the state-space matrixes can be achieved and the eigenvalue trajectories can be plotted for the stability analysis.

TABLE I. Parameters of The Grid-Connected Converter

Grid Parameters		
u_g	Grid voltage	86.6 V
f_g	Grid frequency	50 Hz
SCR	Short-circuit ratio	2.5/10.0
X/R	Ratio of the reactance to resistance	0.1-10
ω_g	Grid angular frequency	314 rad/s
Converter Parameters		
u_{dc}	DC-side voltage	600 V
L_f	Filter inductance	3 mH
C_f	Filter capacitance	20 μF
P_{ref}	Rated active power	1.5 kW
Q_{ref}	Rated reactive power	0 kVar
T_s	Switching period	100 μs
T_{sa}	Sampling period	50 μs
Control Parameters for grid-following converter		
ω_{pll}	Bandwidth of phase-locked loop	13.4 rad/s
ω_{PQ}	Bandwidth of power loop	110 rad/s
ω_i	Bandwidth of current loop	1030 rad/s
K_C	Proportional gain of capacitor current feedback	1
ω_c	Cut-off frequency of LPF	100 rad/s
Control Parameters for grid-forming converter		
ω_u	Bandwidth of voltage loop	23.4 rad/s
ω_i	Bandwidth of current loop	1030 rad/s
K_C	Proportional gain of capacitor current feedback	1
ω_c	Cut-off frequency of LPF	100 rad/s
D	Damping coefficient	50
J	Virtual inertia	0.1 kg/m^2
k_u	Q-U loop coefficient	50
k_q	Integrity coefficient	0.2
E_0	No-load electromotive force of the converter	70.7 V
U_N	Peak value of the rated grid voltage	70.7 V

With the X/R ratio increasing from 0.1 to 10, when the power grid is weak and the SCR is 2.5, the eigenvalues trajectories of the GFL converter and GFM converter are plotted in Fig. 4 and Fig. 5. It can be seen that, when the X/R ratio is larger than 7.4, the dominant eigenvalues λ_1 and λ_2 of

the GFL converter move towards the right half plane, which means the system becomes unstable. For the GFM control, the dominant eigenvalues λ_1 and λ_2 move towards the right half plane with the increase of the X/R ratio, which reveals that the stability of the GFM converter deteriorates. However, all the eigenvalues of the GFM converter are in the left plane. The analysis result reveals that the increase of the X/R ratio deteriorates the stability of both the GFL and GFM converters under the weak power grid. Moreover, in the case of a weak power grid, the X/R ratio has a greater impact on the GFL converter compared to the GFM converter.

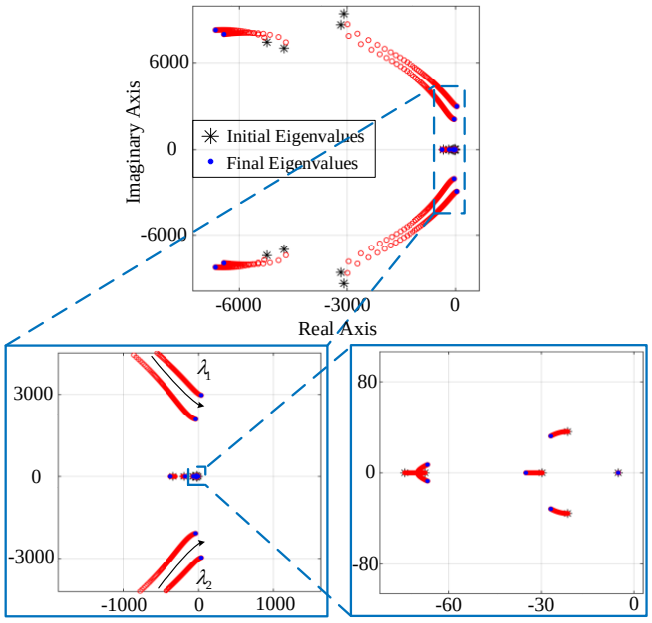

Fig. 4. Eigenvalue trajectories of the grid-following (GFL) converter when the X/R ratio is varied from 0.1 (Initial) to 10 (Final) under a weak grid.

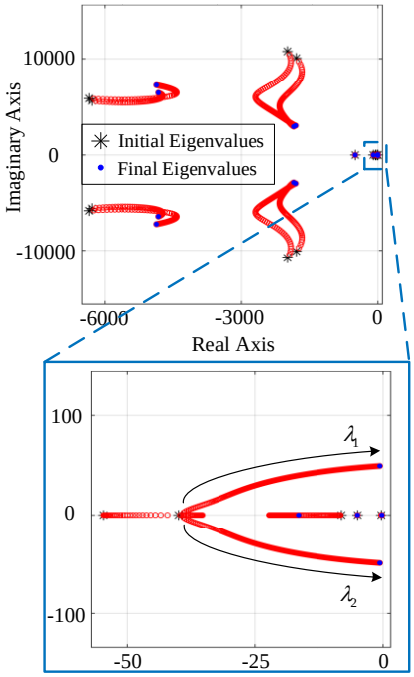

Fig. 5. Eigenvalue trajectories of the grid-forming (GFM) converter when the X/R ratio is varied from 0.1 (Initial) to 10 (Final) under a weak grid.

Similarly, with the X/R ratio increasing from 0.1 to 10, when the power grid is strong and the SCR is 10, the eigenvalues trajectories of the GFL converter and GFM converter are plotted in Fig. 6 and Fig. 7. When the X/R ratio increases, the eigenvalues of the GFL converter move towards right, but all the eigenvalues still stay in the left half plane. However, for the GFM converter, when the X/R ratio is larger than 0.6, the dominant eigenvalues λ_1 and λ_2 move towards the right half plane, which means the system becomes unstable. Thus, the conclusion can be drawn that the increase of the X/R ratio deteriorates the stability of both the GFL and GFM converters under the strong power grid while the X/R ratio has a greater impact on the GFM converter compared to the GFL converter.

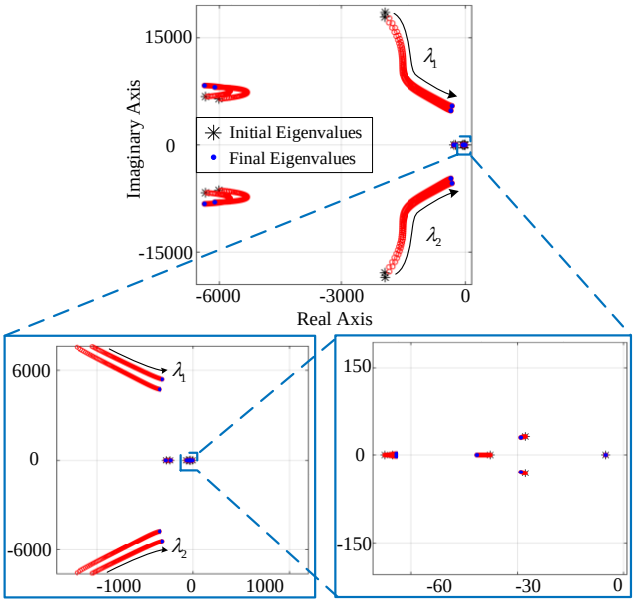

Fig. 6. Eigenvalue trajectories of the grid-following (GFL) converter when the X/R ratio is varied from 0.1 (Initial) to 10 (Final) under a strong grid.

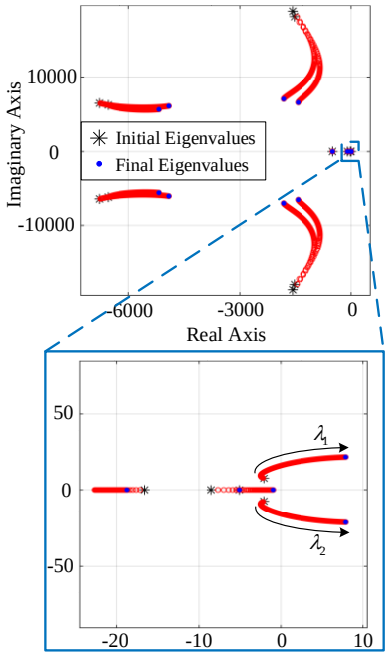

Fig. 7. Eigenvalue trajectories of the grid-forming (GFM) converter when the X/R ratio is varied from 0.1 (Initial) to 10 (Final) under a strong grid.

IV. Simulation Results

In order to verify the aforementioned assessment whether the stability of both the GFL converter and the GFM converter will improve with the decrease of X/R ratio, the time-domain simulation is built in Matlab/Simulink. The parameters are the same as those listed in TABLE I.

The direction of power flows from the converter to the power grid is defined as positive, which is shown in Fig. 8.

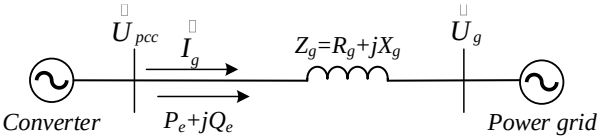

Fig. 8. The power flow between the converter and the power grid.

As shown in Fig. 8, the voltage difference between the PCC and the power grid can be given as:

$$\begin{aligned}\dot{U}_{pcc}-\dot{U}_g &= \dot{I}_g\left(R_g+jX_g\right)\\ &= \frac{P_eR_g+Q_eX_g}{U_g}+j\frac{P_eX_g-Q_eR_g}{U_g}\end{aligned} \tag{2}$$

When the power grid is weak and the SCR is 2.5, the simulation results are shown below. When the X/R ratio increases from 0.1 to 6.5, the references and feedbacks of the output active and reactive power, the PCC voltage, the current loop and the frequency of the GFL converter are shown in Fig. 9. When the X/R ratio increases from 0.1 to 10.0, the references and feedbacks of the power synchronization loop, the excitation loop, the voltage control loop, the current control loop and the frequency of the GFM converter are shown in Fig. 10.

It is worth noting that the d-axis of the PCC voltage u_{pccd} is very high when the X/R ratio is 0.1. With the increase of the X/R ratio, the d-axis of the PCC voltage u_{pccd} decreases which is shown in Fig. 9 and Fig. 10. That is because when the X/R ratio is very small, the reactance effect can be ignored and the amplitude of the PCC voltage can be approximated by:

$$\left|\dot{U}_{pcc}\right| = U_g+\frac{P_eR_g}{U_g} \tag{3}$$

where the effect of the imaginary component is ignored [16] and the amplitude of the PCC voltage is equal to the d-axis of the PCC voltage u_{pccd} because the u_{pccq} is equal to 0.

Moreover, the output active power is controlled as constant and it can be given as:

$$P_e = 1.5\left(u_{pccd}i_d+u_{pccq}i_q\right) \tag{4}$$

Therefore, the i_d increases with the X/R ratio increasing because of the decrease of the u_{pccd}. The GFL converters only regulate the power injected to the power grid, so both the active power and reactive power are constant which is shown in Fig. 9. However, as for the GFM converters, there is a droop relationship between the PCC voltage and the output reactive power because of the excitation loop. Thus, with the decrease of the PCC voltage u_{pccd}, the reactive power Q_e increases.

As shown in Fig. 9, when the X/R ratio increases to 6.5, the GFL converter cannot maintain stable any more, which reveals that the stability of the GFL converter deteriorated with the increase of the X/R ratio. As shown in Fig. 10, the GFM converter can stay stable when the X/R ratio increases from 0.1 to 10.0. However, it may take a longer time to return to stable operation with the increase of the X/R ratio. Thus, it can be concluded that the increase of the X/R ratio deteriorates the stability of both the GFL and GFM converters under the weak power grid while the X/R ratio has a greater impact on the GFL converter compared to the GFM converter.

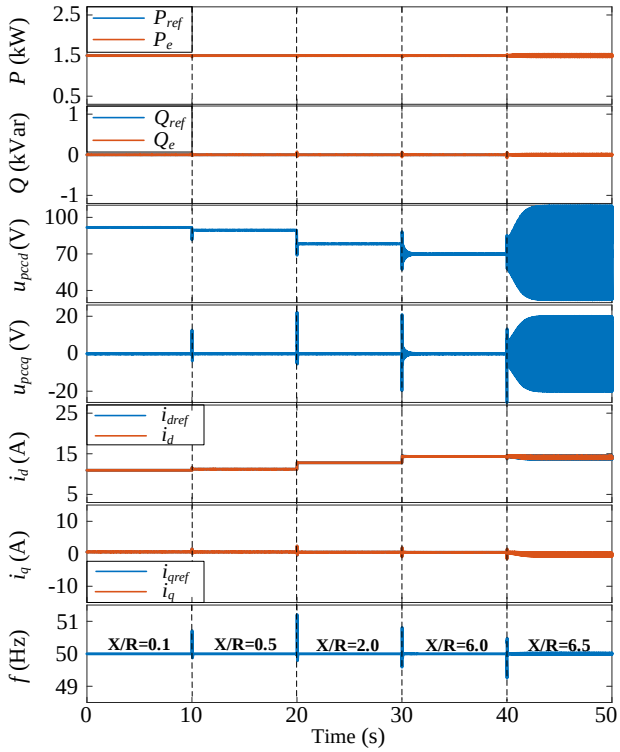

Fig. 9. Simulation results of the grid-following (GFL) converter when the X/R ratio is varied from 0.1 to 6.5 under a weak grid.

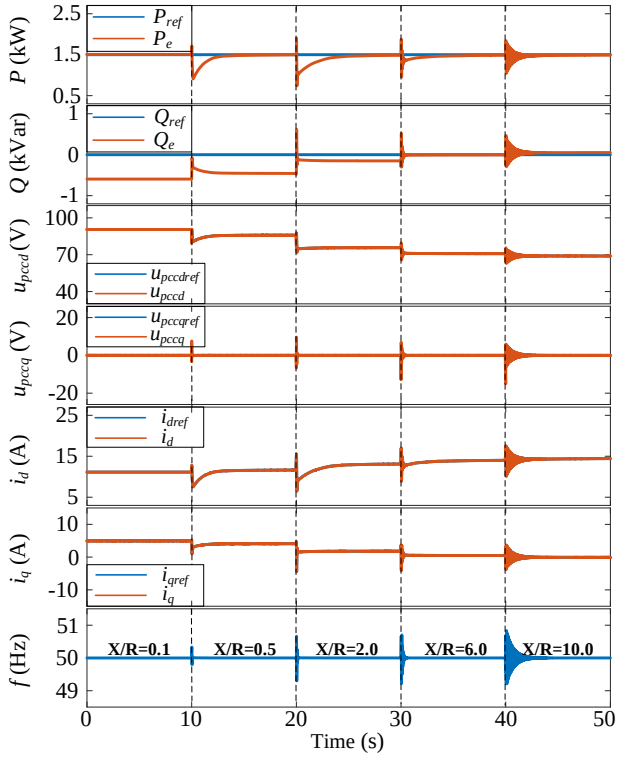

Fig. 10. Simulation results of the grid-forming (GFM) converter when the X/R ratio is varied from 0.1 to 10.0 under a weak grid.

Similarly, when the power grid is strong and the SCR is 10, the simulation results are shown below. When the X/R ratio increases from 0.1 to 10.0, the references and feedbacks of the output active and reactive power, the PCC voltage, the current loop and the frequency of the GFL converter are shown in Fig. 11Fig. 9. When the X/R ratio increases from 0.1 to 0.6, the references and feedbacks of the power synchronization loop, the excitation loop, the voltage control loop, the current control loop and the frequency of the GFM converter are shown in Fig. 12.

As shown in Fig. 11Fig. 9, when the X/R ratio increases from 0.1 to 10.0, the GFL converter stays stable. However, the GFM converter cannot maintain stable when the X/R ratio is larger than 0.5, which is shown in Fig. 12. Thus, it can be concluded that the increase of the X/R ratio deteriorates the stability of GFM converters under the strong power grid and the X/R ratio has a greater impact on the GFM converter compared to the GFL converter.

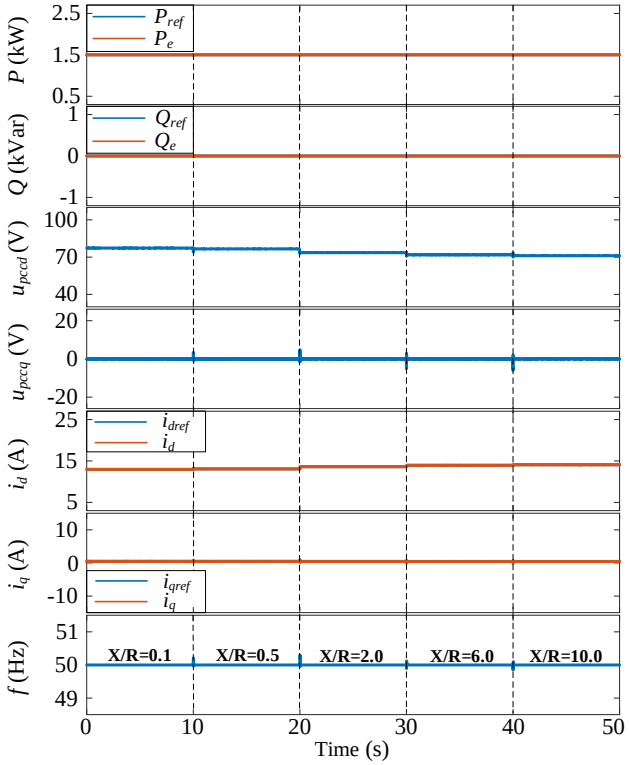

Fig. 11. Simulation results of the grid-following (GFL) converter when the X/R ratio is varied from 0.1 to 10.0 under a strong grid.

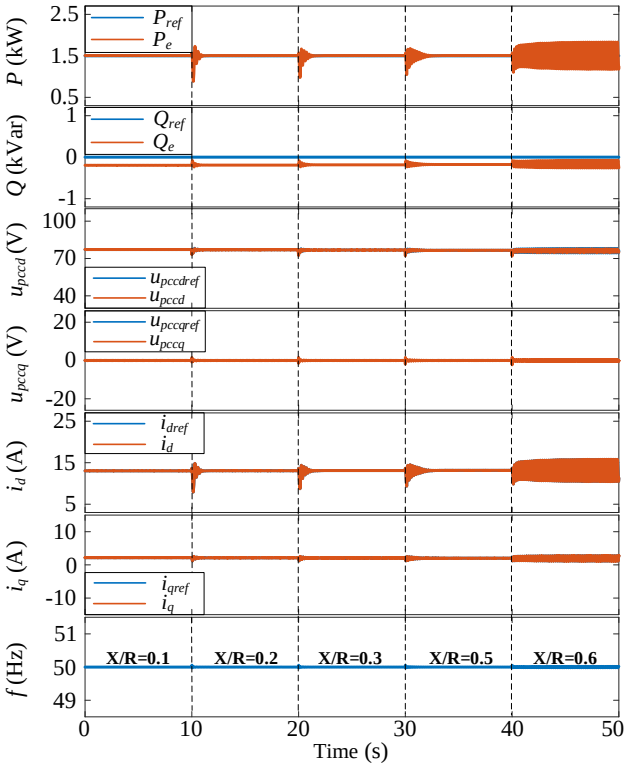

Fig. 12. Simulation results of the grid-forming (GFM) converter when the X/R ratio is varied from 0.1 to 0.6 under a strong grid.

V. Conclusions

This paper provided important insights into the GFL and GFM converters and advanced the understanding of the relationship between the X/R ratio and the stability of power systems. The results from the theoretical analysis of eigenvalue trajectories based on the state-space matrix were consistent with that from the time-domain simulation conducted in Matlab/Simulink. It indicated that the stability of both the GFL and GFM converters will deteriorate with the increase of the X/R ratio. Moreover, the X/R ratio has a greater impact on the GFL converter under a weak power grid, while the X/R ratio has a greater impact on the GFM converter under a strong power grid.

VI. References

[1] X. Gao, D. Zhou, A. Anvari-Moghaddam and F. Blaabjerg, "Stability Analysis of Grid-Following and Grid-Forming Converters Based on State-Space Model," *in Proc. 10th Int. Conf. Power Electron. ECCE Asia*, Himeji, Japan, pp. 422-428, 2022.

[2] G. Wu et al., "Parameter Design Oriented Analysis of the Current Control Stability of the Weak-Grid-Tied VSC," *IEEE Trans. Power Del.*, vol. 36, no. 3, pp. 1458-1470, June 2021.

[3] Y. Liao, X. Wang and F. Blaabjerg, "Passivity-Based Analysis and Design of Linear Voltage Controllers For Voltage-Source Converters," *IEEE Open J. Ind. Electron. Society*, vol. 1, pp. 114-126, 2020.

[4] Z. Qu, J. C. -H. Peng, H. Yang and D. Srinivasan, "Modeling and Analysis of Inner Controls Effects on Damping and Synchronizing Torque Components in VSG-Controlled Converter," *IEEE Trans. Energy Convers.*, vol. 36, no. 1, pp. 488-499, Mar. 2021.

[5] H. Gong and X. Wang, "Design-Oriented Analysis of Grid-Forming Control with Hybrid Synchronization," *in Proc. 10th Int. Conf. Power Electron. ECCE Asia*, Himeji, Japan, pp. 440-446, 2022.

[6] R. Yin, Y. Sun, S. Wang and L. Zhang, "Stability Analysis of the Grid-Tied VSC Considering the Influence of Short Circuit Ratio and X/R," *IEEE Trans. Circuits Sys. II, Exp. Briefs*, vol. 69, no. 1, pp. 129-133, Jan. 2022.

[7] R. Yin, et al. "Modeling and stability analysis of grid-tied VSC considering the impact of voltage feed-forward." *Int. J. Electron. Power Energy Syst.*, vol. 135, pp. 1–12, Feb., 2022.

[8] L. Huang, C. Wu, D. Zhou, and F. Blaabjerg, "Impact of grid strength and impedance characteristics on the maximum power transfer capability of grid-connected inverters," *Appl. Sci.*, vol. 11, no. 9, pp. 1–15, May 2021.

[9] N. Pogaku, M. Prodanovic and T. C. Green, "Modeling, Analysis and Testing of Autonomous Operation of an Inverter-Based Microgrid," *IEEE Trans. Power Electron.*, vol. 22, no. 2, pp. 613-625, March 2007.

[10] J. Sun, "Impedance-Based Stability Criterion for Grid-Connected Inverters," *IEEE Trans. Power Electron.*, vol. 26, no. 11, pp. 3075-3078, Nov. 2011.

[11] A. Hadjileonidas, Y. Li and T. C. Green, "Comparative Analysis of Transient Stability of Grid-Forming and Grid-Following Inverters," *in Proc. IEEE Int. Power Electron. Appl. Conf. Expo., (PEAC)*, Guangzhou,Guangdong, China, pp. 296-301, 2022.

[12] S. Golestan, M. Ramezani, J. M. Guerrero, F. D. Freijedo and M. Monfared, "Moving Average Filter Based Phase-Locked Loops: Performance Analysis and Design Guidelines," *IEEE Trans. Power Electron.*, vol. 29, no. 6, pp. 2750-2763, June 2014.

[13] B. Wen, D. Boroyevich, R. Burgos, P. Mattavelli, and Z. Shen, "Analysis of D-Q Small-Signal Impedance of Grid-Tied Inverters," *IEEE Trans. Power Electron.*, vol. 31, no. 1, pp. 675-687, Jan. 2016.

[14] X. Gao, D. Zhou, A. Anvari-Moghaddam and F. Blaabjerg, "A Comparative Study of Grid-Following and Grid-Forming Control Schemes in Power Electronic-Based Power Systems," *Power Electronics and Drives*, vol. 8, no. 1, pp. 1-20, Jan. 2023.

[15] *IEEE Guide for Planning DC Links Terminating at AC Locations Having Low Short-Circuit Capacities*, Standard 1204-1997, IEEE, New York, NY, USA, 1997.

[16] G. Yang et al., "Voltage rise mitigation for solar PV integration at LV grids Studies from PVNET. dk," *J. Modern Power Syst. Clean Energy*, vol. 3, no. 3, pp. 411-421, September 2015.